

# LDDMM meets GANs: Generative Adversarial Networks for diffeomorphic registration

Ubaldo Ramon, Monica Hernandez, and Elvira Mayordomo

Computer Sciences Department  
Aragon Institute on Engineering Research  
University of Zaragoza  
{uramon,mhg,elvira}@unizar.es

**Abstract.** The purpose of this work is to contribute to the state of the art of deep-learning methods for diffeomorphic registration. We propose an adversarial learning LDDMM method for pairs of 3D mono-modal images based on Generative Adversarial Networks. The method is inspired by the recent literature for deformable image registration with adversarial learning. We combine the best performing generative, discriminative, and adversarial ingredients from the state of the art within the LDDMM paradigm. We have successfully implemented two models with the stationary and the EPDiff-constrained non-stationary parameterizations of diffeomorphisms. Our unsupervised and data-hungry approach has shown a competitive performance with respect to a benchmark supervised and rich-data approach. In addition, our method has shown similar results to model-based methods with a computational time under one second.

**Keywords:** Large Deformation Diffeomorphic Metric Mapping , Generative Adversarial Networks , geodesic shooting , stationary velocity fields.

## 1 Introduction

Since the 80s, deformable image registration has become a fundamental problem in medical image analysis [1]. A vast literature on deformable image registration methods exist, providing solutions to important clinical problems and applications. Up to the ubiquitous success of methods based on Convolutional Neural Networks (CNNs) in computer vision and medical image analysis, the great majority of deformable image registration methods were based on energy minimization models [2]. The problem of computing the deformation that *best* warps the source into the target image was solved from the minimization of a variational problem involving different ingredients such as the deformation parameterization, the regularization and image similarity metrics, and the optimization method used in the minimization of the energy. This traditional approach is model-based, in contrast with recent deep-learning approaches that are known as data-based.

Diffeomorphic registration constitutes the inception point in Computational Anatomy studies for modeling and understanding population trends and longitudinal variations, and for establishing relationships between imaging phenotypes and genotypes in Imaging Genetics [3, 4]. Model-based diffeomorphic image registration is computationally costly. In fact, the huge computational complexity of large deformation diffeomorphic metric mapping (LDDMM) [5] is considered the curse of diffeomorphic registration, where very original solutions such as the stationary parameterization [6–8], the EPDiff constraint on the initial velocity field [9], or the band-limited parameterization [10] have been proposed to alleviate the problem.

Since the advances that made it possible to learn the optical flow using CNNs (FlowNet [11]), dozens of deep-learning data-based methods have been proposed to approach the problem of deformable image registration in different clinical applications [12]. The trend is augmenting considerably in the last three years. From them, some interesting proposals have been performed for diffeomorphic registration [13–19]. These proposals still use most of the ingredients of traditional model-based methods such as the stationary parameterization [13, 15, 17, 16], the non-stationary parameterization, the parameterization with EPDiff-constrained velocity fields [14, 19], the LDDMM energy regularization, and traditional image similarity metrics. The network architectures are based on ensembles of fully convolutional (FC) layers [13–15, 19] or modified U-Net based architectures [18], where the input data varies between image patches [14] and the whole image [18].

All the proposals to diffeomorphic registration can be classified into supervised [13, 14, 19] or unsupervised learning methods [15, 17, 18]. Unsupervised methods are usually preferred over supervised ones since the transformations can be learned directly from image pairs, avoiding the overhead to compute ground truth transformations for training, which is usually approached going back to model-based methods. Overall, all data-based methods yield fast inference algorithms for diffeomorphism computation once the difficulties with training have been overcome.

Generative Adversarial Networks (GANs) is an interesting unsupervised approach and, to our knowledge, it has not been yet proposed in the framework of diffeomorphic registration. In fact, GANs for deformable registration can be considered at its infancy with few but interesting proposals like [20] (2D) and [21, 22] (3D). A GAN combines the interaction of two different networks during training: a generative network and a discrimination network. The generative network itself can be regarded as an unsupervised method that, once included in the GAN system, is trained with the feedback of the discrimination network. It is expected that the generator converges faster and more precisely since the discriminator urges to produce pairs of images indistinguishable from the real distribution of target and warped source image pairs.

The purpose of this work is to contribute to the state of the art of data-based methods for diffeomorphic registration and propose an adversarial learning LDDMM method for pairs of 3D mono-modal images. The method is inspired in

the recent literature for deformable image registration with adversarial learning [21, 22]. Indeed, it combines the best performing generative, discriminative, and adversarial ingredients from these works within the LDDMM paradigm. We have successfully implemented two models for the stationary and the EPDiff-constrained non-stationary parameterizations. We demonstrate the effectiveness of our models in both 2D simulated and 3D real brain MRI data.

In the following, Section 2 reviews the foundations of LDDMM underpinning in this work. Section 3 describes the proposed method. Section 4 describes the datasets used for the training and evaluation of our method and shows the quantitative and qualitative evaluation results. Finally, Section 5 derives some interesting conclusions of our work.

## 2 Background on LDDMM

Let  $\Omega \subseteq \mathbb{R}^d$  be the image domain. Let  $Diff(\Omega)$  be the LDDMM Riemannian manifold of diffeomorphisms and  $V$  the tangent space at the identity element.  $Diff(\Omega)$  is a Lie group, and  $V$  is the corresponding Lie algebra [5]. The Riemannian metric of  $Diff(\Omega)$  is defined from the scalar product in  $V$ ,  $\langle v, w \rangle_V = \langle Lv, w \rangle_{L^2}$ , where  $L$  is the invertible self-adjoint differential operator associated with the differential structure of  $Diff(\Omega)$ . In traditional LDDMM methods,  $L = (Id - \alpha \Delta)^s$ ,  $\alpha > 0$ ,  $s \in \mathbb{R}$  [5]. We will denote with  $K$  the inverse of operator  $L$ .

Let  $I_0$  and  $I_1$  be the source and the target images. LDDMM is formulated from the minimization of the variational problem

$$E(v) = \frac{1}{2} \int_0^1 \langle Lv_t, v_t \rangle_{L^2} dt + \frac{1}{\sigma^2} \|I_0 \circ (\phi_1^v)^{-1} - I_1\|_{L^2}^2. \quad (1)$$

The LDDMM variational problem was originally posed in the space of time-varying smooth flows of velocity fields,  $v \in L^2([0, 1], V)$ . Given the smooth flow  $v : [0, 1] \rightarrow V$ ,  $v_t : \Omega \rightarrow \mathbb{R}^d$ , the solution at time  $t = 1$  to the evolution equation

$$\partial_t (\phi_t^v)^{-1} = -v_t \circ (\phi_t^v)^{-1} \quad (2)$$

with initial condition  $(\phi_0^v)^{-1} = id$  is a diffeomorphism,  $(\phi_1^v)^{-1} \in Diff(\Omega)$ . The transformation  $(\phi_1^v)^{-1}$ , computed from the minimum of  $E(v)$ , is the diffeomorphism that solves the LDDMM registration problem between  $I_0$  and  $I_1$ .

The most significant limitation of LDDMM is its large computational complexity. In order to circumvent this problem, the original LDDMM variational problem is parameterized on the space of initial velocity fields

$$E(v_0) = \frac{1}{2} \langle Lv_0, v_0 \rangle_{L^2} + \frac{1}{\sigma^2} \|I_0 \circ (\phi_1^v)^{-1} - I_1\|_{L^2}^2. \quad (3)$$

where the time-varying flow of velocity fields  $v$  is obtained from the EPDiff equation

$$\partial_t v_t + K[(Dv_t)^T \cdot Lv_t + DLv_t \cdot v_t + Lv_t \cdot \nabla \cdot v_t] = 0 \quad (4)$$

with initial condition  $v_0$  (geodesic shooting). The diffeomorphism  $(\phi_1^v)^{-1}$ , computed from the minimum of  $E(v_0)$  via Equations 4 and 2, verifies the momentum conservation constraint (MCC) [23], and, therefore, it belongs to a geodesic path on  $Diff(\Omega)$ .

Simultaneously to the MCC parameterization, a family of methods was proposed to further circumvent the large computational complexity of original LDDMM [6–8]. In all these methods, the time-varying flow of velocity fields  $v$  is restricted to be steady or stationary [24].

### 3 Generative Adversarial Networks for LDDMM

#### 3.1 GAN-based unsupervised deep-learning networks for diffeomorphic registration

Similarly to model-driven approaches for estimating LDDMM diffeomorphic registration, data-driven approaches for learning LDDMM diffeomorphic registration aim at the inference of a diffeomorphism  $(\phi_1^v)^{-1}$  such that the LDDMM energy is minimized for a given  $(I_0, I_1)$  pair. In particular, data-driven approaches compute an approximation of the functional

$$\mathcal{S}(\arg \min_{v \in V} E(v, I_0, I_1)) \quad (5)$$

where  $\mathcal{S}$  represents the operations needed to compute  $(\phi_1^v)^{-1}$  from  $v$ , and the energy  $E$  is either given by Equations 1 or 3. The functional approximation is obtained via a neural network representation with parameters learned from a representative sample of image pairs. Unsupervised approaches assume that the LDDMM parameterization in combination with the minimization of the energy  $E$  considered as a loss function are enough for the inference of suitable diffeomorphic transformations after training. Therefore, there is no need for ground truth deformations.

GAN-based approaches depart from unsupervised approaches by the definition of two different networks: the generative network (G) and the discrimination network (D). These networks are trained in an alternating way in an adversarial fashion. The generative network in this context is the diffeomorphic registration network. G is aimed at the approximation of the functional given in Equation 5 similarly to unsupervised approaches for the inference of  $(\phi_1^v)^{-1}$ . The discrimination network D outputs the probability  $p \in [0, 1]$  that for a pair  $(I_0^w, I_1)$  the image  $I_0^w$  comes from a warped source *not* being generated by G.

The discrimination network D learns to distinguish between a warped source image  $I_0 \circ (\phi_1^v)^{-1}$  generated by G and a plausible warped source image. The learnable parameters of the network G are trained to minimize traditional LDDMM cost functions between the warped source image and the target image while trying to fool the discriminator D. In contrast to other unsupervised approaches, the loss function in G is determined from the combination of the LDDMM and the adversarial costs.

### 3.2 Adversarial training

As stated above, the registration architecture is composed of two neural networks, a generator G and a discriminator D, which are trained alternatively as follows.

The discriminator network D is trained using the loss function

$$L_D = \begin{cases} -\log(p) & c \in P^+ \\ -\log(1-p) & c \in P^- \end{cases} \quad (6)$$

where  $c$  indicates the input case,  $P^+$  and  $P^-$  indicate positive or negative cases for the GAN, and  $p$  is the probability computed by D for the input case.

In the first place, D is trained on a positive case  $c \in P^+$  representing a target image  $I_1$  and a warped source image  $I_0^w$  plausibly registered to  $I_1$  with a diffeomorphic transformation. The warped source image is modeled from a strictly convex linear combination of  $I_0$  and  $I_1$   $I_0^w = \beta I_0 + (1 - \beta)I_1$ . It should be noticed that, although the warped source image would ideally be  $I_1$ , the selection of  $I_0^w = I_1$  (e.g.  $\beta = 0$ ) empirically leads to the discriminator rapidly outperforming the generator. The parameter  $\beta$  is the relative *MSE* error obtained after registration for  $I_0^w$  and  $I_1$  since

$$MSE_{rel} = \frac{\|I_0 \circ (\phi_1^v)^{-1} - I_1\|_{L^2}^2}{\|I_0 - I_1\|_{L^2}^2} \text{ and } \|I_0^w - I_1\|_{L^2}^2 = \beta \|I_0 - I_1\|_{L^2}^2. \quad (7)$$

Therefore, this model for  $I_0^w$  can be regarded a good candidate for warped sources after deformable registration for small  $\beta$ s. It has been successfully used in adversarial learning methods for deformable registration [22].

In the second place, D is trained on a negative case  $c \in P^-$  representing a target image  $I_1$  and a warped source image  $I_0^w$  obtained from the generator network G.

In third place, the generator network G is trained using the combined loss function

$$L_G = L_{adv} + \lambda E(v, I_0, I_1). \quad (8)$$

In this loss function,  $L_{adv}$  is the adversarial loss function, defined from  $L_{adv} = -\log(p)$  where  $p$  is computed from D;  $E$  is the LDDMM energy given by Equations 1 or 3; and  $\lambda$  is the weight for balancing the adversarial and the generative losses. For each sample pair  $(I_0^w, I_1)$ , G is fed with the pair of images and updates the network parameters from the back-propagation of the information of the loss function values coming from the LDDMM energy and the discriminator probability of being a pair generated by G.

In the early stages of learning, it is expected that the generator network provides misaligned images and the discriminator penalizes the system with high probabilities for the negative cases. As the learning progresses, the generator is trained to fool the discriminator, so the generated warped sources will be diffeomorphically transformed to resemble  $I_1$  as much as possible according to the convex linear model. The discrimination will eventually hardly distinguish the generated warped sources from the true population, yielding low probabilities for the negative cases, and learning will be considered to converge.

### 3.3 Proposed GAN architecture

**Generator network.** In this work, the diffeomorphic registration network G is intended to learn LDDMM diffeomorphic registration parameterized on the space of steady velocity fields or the space of initial velocity fields subject to the EPDiff equation (Equation 4). The diffeomorphic transformation  $(\phi_1^v)^{-1}$  is obtained from these velocity fields either from scaling and squaring [7, 8] or the solution of the deformation state equation [5]. Euler integration is used as PDE solver for all the involved differential equations.

A number of different generator network architectures have been proposed in the recent literature, with predominance of simple fully convolutional (FC) [20] or U-Net like architectures [21, 22]. In this work, we propose to use the architecture by Duan et al. [21] adapted to fit our purposes. The network follows the general U-net design of utilizing a encoder- decoder structure with skip connections. However, during the encoding phase, the source and target images are fed to two encoding streams. The first stream follows a fully convolutional design (FC) while the second stream follows the traditional U-net encoding pattern. For each resolution level, the parameters from the two streams are combined and fed to the next level. In contrast to simpler U-net architectures, the combination of the two encoding streams allows a larger receptive field suitable to learn large deformations. During the decoding phase, the encoding output is passed through an upsampling decoder to obtain the velocity field and the diffeomorphic transformation  $(\phi_1^v)^{-1}$ . The upsampling is performed with a deconvolutional operation based on transposed convolutional layers [25]. We have empirically noticed that the learnable parameters of these layers help reducing typical checkerboard GAN artifacts in the decoding [26].

**Discriminator network.** The discriminator network D follows a very traditional CNN architecture. The two input images are concatenated and passed through five convolutional blocks. Each block includes a convolutional layer, a RELU activation function, and a size-two max-pooling layer. After the convolutions, the 4D volume is flattened and passed through three fully connected layers. The output of the last layer is the probability of the input images to come from a registered pair not generated by G.

**Generative-Discriminative integration layer.** The generator and the discriminator networks G and D are connected through an integration layer in the shape of a spatial transformation layer. This integration layer allows calculating the diffeomorphism  $(\phi_1^v)^{-1}$  that warps the source image  $I_0$ . The selected integration layer depends on the velocity parameterization: stationary or EPDiff-constrained time-dependent. The computed diffeomorphisms are applied to the source image via a second 3D spatial transformation layer [27] with no learnable parameters. The gradients of the integration layer are back-propagated from D to train G. In the following, the method with the stationary parameterization will be recalled as SVF-GAN, and the method with the EPDiff-constrained parameterization will be recalled as EPDiff-GAN.

**Parameter selection and implementation details** We selected the parameters  $\lambda = 1000$ ,  $\sigma^2 = 1.0$ ,  $\alpha = 0.0025$ , and  $s = 4$  and a unit-domain discretization of the image domain  $\Omega$  [5]. Scaling and squaring and Euler integration were performed in 10 time samples. The parameter  $\beta$  for the convex linear modeling of warped images was selected equal to 0.2. This means that the discriminator is trained to learn deformable image registration results with a 20% of  $MSE_{rel}$  level of accuracy.

Both the generator network and the discriminator network were trained with Adam’s optimizer with default parameters and learning rates of  $5e^{-5}$  for G and  $1e^{-6}$  for D, respectively.

The experiments were run on a machine equipped with one NVidia Titan RTX with 24 GBS of video memory and an Intel Core i7 with 64 GBS of DDR3 RAM. The codes were developed in the GPU with Keras and a TensorFlow backend.

## 4 Results

In this section we demonstrate the effectiveness of our non-supervised proposed methods by training and testing on a 2D simulated dataset and 3D brain MRI datasets.

### 4.1 Datasets

**2D simulated dataset.** We simulated a total of 2560 torus images by varying the parameters of two ellipse equations, similarly to [19]. The parameters were drawn from two Gaussian distributions:  $\mathcal{N}(4, 2)$  for the inner ellipse and  $\mathcal{N}(12, 4)$  for the outer ellipse. The simulated images were of size  $64 \times 64$ . Our GANs were trained during 1000 epochs with a batch size of 64 samples.

**3D brain MRI datasets.** For adversarial training, we used a total of 2113 T1-weighted brain MRI images from the Alzheimer’s Disease Neuroimaging Initiative (ADNI,adni.loni.usc.edu). The ADNI was launched in 2003 as a public-private partnership, led by Principal Investigator Michael W. Weiner, MD. The primary goal of ADNI has been to test whether serial magnetic resonance imaging (MRI), positron emission tomography (PET), other biological markers, and clinical and neuropsychological assessment can be combined to measure the progression of mild cognitive impairment (MCI) and early Alzheimer’s disease (AD). The images were acquired at the baseline visit and belong to all the available ADNI projects (1, 2, Go, and 3). The images were preprocessed with N3 bias field correction, affinely registered to the MNI152 atlas, skull-stripped, and affinely registered to the skull-stripped MNI152 atlas.

The evaluation of our generated GAN models in the task of diffeomorphic registration was performed in NIREP dataset [28]. This dataset was released for the evaluation of non-rigid registration. The geometry of the segmentations

in NIREP provides a specially challenging framework for deformable registration evaluation. The images were acquired from 8 males and 8 females with a mean age of  $32.5 \pm 8.4$  and  $29.8 \pm 5.8$  years, respectively. The substantial age differences between train and test subjects are intended to demonstrate the generalization capability of our non-supervised models.

Both the encoder and decoder networks in G were implemented to work with images of size  $176 \times 224 \times 176$ . Our GANs were trained during 50 epochs with a batch size of 1 sample. This selection of image size and batch sampling was performed due to VRAM memory issues.

## 4.2 Results in the 2D simulated dataset

Figure 1 shows the deformed images and the velocity fields obtained in the 2D simulated dataset by diffeomorphic Demons [7], a stationary version of LDDMM (St. LDDMM) [8], the spatial version of Flash [10], and our proposed SVF and EPDiff GANs. Apart from diffeomorphic Demons that uses Gaussian smoothing for regularization, all the considered methods use the same parameters for operator  $L$ . Therefore, St. LDDMM and SVF-GAN can be seen as a model-based and a data-based approach for the minimization of the same variational problem. The same happens with Flash and EPDiff-GAN.

From the figure, it can be appreciated that our proposed GANs are able to obtain accurate warps of the source to the target images, similarly to model-based approaches. For SVF-GAN, the inferred velocity fields are visually similar to model-based approaches in three of five experiments. For EPDiff-GAN, the inferred initial velocity fields are visually similar to model-based approaches in four of five experiments.

## 4.3 Results in the 3D NIREP dataset

**Quantitative assessment** Figure 2 shows the Dice similarity coefficients obtained with diffeomorphic Demons [7], St. LDDMM [8], Voxelmorph II [16], the spatial version of Flash [10], Quicksilver [14] and our proposed SVF and EPDiff GANs. From them, we show the results of our proposed two-stream architecture in contrast to a simpler U-Net based architecture. The results have been split into stationary and geodesic shooting methods.

From the figure, it can be appreciated that our proposed two-stream architecture greatly improves the accuracy obtained by simple U-Net. SVF-GAN shows an accuracy similar to St. LDDMM and competitive with diffeomorphic Demons. Our proposed method tends to overpass Voxelmorph II in the great majority of the structures. On the other hand, EPDiff-GAN shows an accuracy similar to Flash and Quicksilver in the great majority of regions, with the exception of the temporal pole (TP) and the orbital frontal gyrus (OFG), two small localized and difficult to register regions. It drives our attention that Flash underperformed in the superior frontal gyrus (SFG).



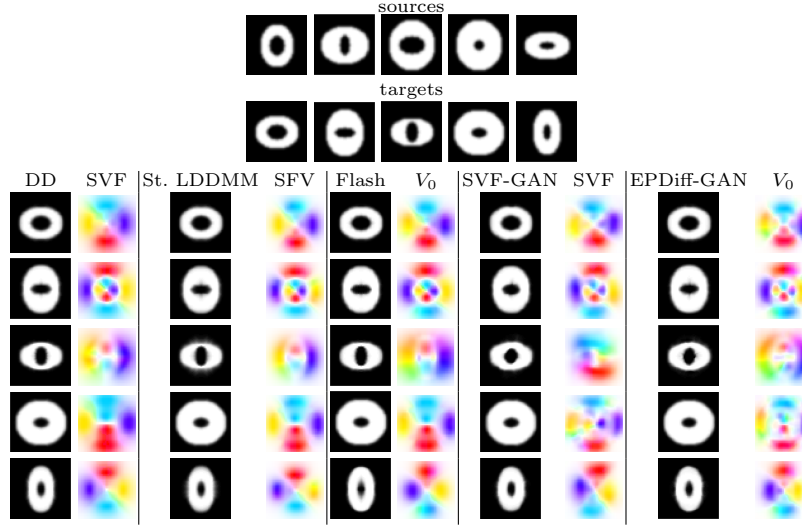


**Fig. 1.** Example of simulated 2D registration results. Up: source and target images of five selected experiments. Down, left to right: deformed images and velocity fields computed from diffeomorphic Demons (DD), stationary LDDMM (St. LDDMM), Flash, and our proposed SVF-GAN and EPDiff-GAN. SVF stands for a stationary velocity field and  $V_0$  for the initial velocity field of a geodesic shooting approach, respectively.

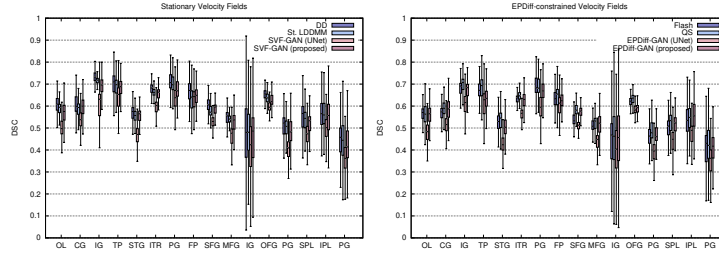


**Fig. 2.** Evaluation in NIREP. Dice scores obtained by propagating the diffeomorphisms to the segmentation labels on the 16 NIREP brain structures. Left, methods parameterized with stationary velocity fields: diffeomorphic Demons (DD), stationary LDDMM (St. LDDMM), Voxelmorph II, our SVF-GAN with U-Net architecture, and our proposed SFV-GAN with the two-stream architecture. Right, geodesic shooting methods: Flash, Quicksilver (QS), our EPDiff-GAN with U-Net architecture, and our proposed EPDiff-GAN.

**Qualitative assessment** For a qualitative assessment of the quality of the registration results, Figure 3 shows the sagittal and axial views of one selected NIREP registration result. In the figure, it can be appreciated a high matching between the target and the warped ventricles, and more difficult to register regions like the cingulate gyrus (observable in the sagittal view) or the insular cortex (observable in the axial view). For those not familiar with brain anatom-

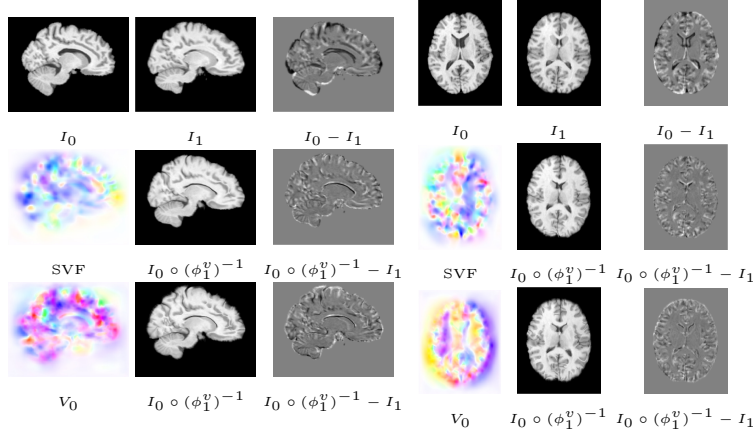


**Fig. 3.** Example of 3D registration results. First row, sagittal and axial views of the source and the target images and the differences before registration. Second row, inferred stationary velocity field, warped image, and differences after registration for SVF-GAN. Third row, inferred initial velocity field, warped image, and differences after registration for EPDiff-GAN.

ical regions, these regions are easily identified as the garnet and orange regions in <https://radiopaedia.org/cases/brain-lobes-annotated-mri-1>.

**Computational complexity** Our GANs models were trained during 2 days, 21 hours, 59 minutes and 48 seconds. The VRAM memory load was equal to the whole GPU capacity. The inference of a stationary or an initial velocity field took 1.3 seconds.

## 5 Conclusions

We have proposed an adversarial learning LDDMM method for the registration of 3D mono-modal images. Our method is inspired by the recent literature on deformable image registration with adversarial learning and combines the best performing generative, discriminative, and adversarial ingredients from these works within the LDDMM paradigm. We have successfully implemented two models: one for the stationary parameterization and the other for the EPDiff-constrained non-stationary parameterization (geodesic shooting).

Our experiments have shown that the inferred velocity fields are comparable to the solutions of model-based approaches. In addition, the evaluation study has shown the competitiveness of our approach with state of the art model- and data- based methods. It should be remarked that our methods perform similarly to Quicksilver, a supervised method that uses patches for training, and therefore, it learns in a rich-data environment. In contrast, our method is unsupervised and uses the whole image for training in a data-hungry environment.

Despite the apparent disadvantages, the evaluation only reported the weakness of EPDiff-GAN in the registration of two regions that are located in challenging locations. Indeed, our proposed methods outperform Voxelmorph II, a regular (not GAN) unsupervised method for diffeomorphic registration usually selected as benchmark in the state of the art.

Once the training has been completed, our method shows a computational time of over a second for the inference of velocity fields. Therefore, our proposal may constitute a good candidate for the massive computation of diffeomorphisms in Computational Anatomy studies.

## Acknowledgements

\*Data used in preparation of this article were obtained from the Alzheimer’s Disease Neuroimaging Initiative (ADNI) database ([adni.loni.usc.edu](http://adni.loni.usc.edu)). As such, the investigators within the ADNI contributed to the design and implementation of ADNI and/or provided data but did not participate in analysis or writing of this report. A complete listing of ADNI investigators can be found at: [http://adni.loni.usc.edu/wp-content/uploads/how\\_to\\_apply/ADNI\\_Acknowledgement\\_List.pdf](http://adni.loni.usc.edu/wp-content/uploads/how_to_apply/ADNI_Acknowledgement_List.pdf)

Data collection and sharing for this project was funded by the Alzheimer’s Disease Neuroimaging Initiative (ADNI) (National Institutes of Health Grant U01 AG024904) and DOD ADNI (Department of Defense award number W81XWH-12-2-0012). ADNI is funded by the National Institute on Aging, the National Institute of Biomedical Imaging and Bioengineering, and through generous contributions from the following: AbbVie, Alzheimer’s Association; Alzheimer’s Drug Discovery Foundation; Araclon Biotech; BioClinica, Inc.; Biogen; Bristol-Myers Squibb Company; CereSpir, Inc.; Cogstate; Eisai Inc.; Elan Pharmaceuticals, Inc.; Eli Lilly and Company; EuroImmun; F. Hoffmann-La Roche Ltd and its affiliated company Genentech, Inc.; Fujirebio; GE Healthcare; IXICO Ltd.; Janssen Alzheimer Immunotherapy Research & Development, LLC.; Johnson & Johnson Pharmaceutical Research & Development LLC.; Lumosity; Lundbeck; Merck & Co., Inc.; Meso Scale Diagnostics, LLC.; NeuroRx Research; Neurotrack Technologies; Novartis Pharmaceuticals Corporation; Pfizer Inc.; Piramal Imaging; Servier; Takeda Pharmaceutical Company; and Transition Therapeutics. The Canadian Institutes of Health Research is providing funds to support ADNI clinical sites in Canada. Private sector contributions are facilitated by the Foundation for the National Institutes of Health ([www.fnih.org](http://www.fnih.org)). The grantee organization is the Northern California Institute for Research and Education, and the study is coordinated by the Alzheimer’s Therapeutic Research Institute at the University of Southern California. ADNI data are disseminated by the Laboratory for Neuro Imaging at the University of Southern California.

## References

1. Sotiras, A., Davatzikos, C., Paragios, N.: Deformable medical image registration: A survey. *IEEE Trans. Med. Imaging* **32(7)** (2013) 1153 – 1190

2. Modersitzki, J.: FAIR: Flexible Algorithms for Image Registration. SIAM (2009)
3. Hua, X., ADNI: Tensor-based morphometry as a neuroimaging biomarker for Alzheimer's disease: an MRI study of 676 AD, MCI, and normal subjects. *Neuroimage* **43(3)** (2008) 458 – 469
4. Liu, Y., Li, Z., Ge, Q., Lin, N., Xiong, M.: Deep feature selection and causal analysis of Alzheimer's disease. *Front. Neurosci.* (2019)
5. Beg, M.F., Miller, M.I., Trounev, A., Younes, L.: Computing large deformation metric mappings via geodesic flows of diffeomorphisms. *Int. J. Comput. Vision* **61(2)** (2005) 139–157
6. Ashburner, J.: A fast diffeomorphic image registration algorithm. *Neuroimage* **38(1)** (2007) 95 – 113
7. Vercauteren, T., Pennec, X., Perchant, A., Ayache, N.: Diffeomorphic Demons: Efficient non-parametric image registration. *Neuroimage* **45(1)** (2009) S61–S72
8. Hernandez, M.: Gauss-Newton inspired preconditioned optimization in large deformation diffeomorphic metric mapping. *Phys. in Med. and Biol.* **59(20)** (2014)
9. Vialard, F.X., Risser, L., Rueckert, D., Cotter, C.J.: Diffeomorphic 3D image registration via geodesic shooting using an efficient adjoint calculation. *Int. J. Comput. Vision* **97(2)** (2011) 229 – 241
10. Zhang, M., Fletcher, T.: Fast diffeomorphic image registration via Fourier-Approximated Lie algebras. *Int. J. Comput. Vision* (2018)
11. Dosovitskiy, A., Fischere, P., Ilg, E., Hausser, P., Hazirbas, C., Golkov, V.: FlowNet: Learning optical flow with convolutional networks. *Proc. of the 16th IEEE International Conference on Computer Vision (ICCV'15)* (2015) 2758 – 2766
12. Boveiri, H., Khayami, R., Javidan, R., Mehdizadeh, A.: Medical image registration using deep neural networks: A comprehensive review. *Computers and Electrical engineering* **87** (2020) 106767
13. Rohe, M.M., Datar, M., Heimann, T., Sermesant, M., Pennec, X.: SVF-Net: Learning deformable image registration using shape matching. *Proc. of the 20th International Conference on Medical Image Computing and Computer Assisted Intervention (MICCAI'17), Lecture Notes in Computer Science* (2017) 266 – 274
14. Yang, X., Kwitt, R., Styner, M., Niethammer, M.: Quicksilver: Fast predictive image registration - a deep learning approach. *Neuroimage* **158** (2017) 378 – 396
15. Dalca, A.V., Blakrishnan, G., Guttag, J., Sabuncu, M.: Unsupervised learning for fast probabilistic diffeomorphic registration. *Proc. of the 21th International Conference on Medical Image Computing and Computer Assisted Intervention (MICCAI'18), Lecture Notes in Computer Science* (2018) 729 – 738
16. Balakrishnan, G., Zhao, A., Sabuncu, M.R., Guttag, J., Dalca, A.V.: Voxelmorph: A learning framework for deformable medical image registration. *IEEE Trans. Med. Imaging* **38(8)** (2019) 1788–1800
17. Krebs, J., Delingetter, H., Mailhe, B., Ayache, N., Mansi, T.: Learning a probabilistic model for diffeomorphic registration. *IEEE Trans. Med. Imaging* (2019)
18. Fan, J., Cao, X., Yap, P., Shen, D.: BIRNet: brain image registration using dual-supervised fully convolutional networks. *Med. Image Anal.* **54** (2019) 193 – 206
19. Wang, J., Zhang, M.: DeepFLASH: an efficient network for learning-based medical image registration. *Proc. of the IEEE Conference on Computer Vision and Pattern Recognition (CVPR'20)* (2020)
20. Mahapatra, D., Antony, B., Sedai, S., Garvani, R.: Deformable medical image registration using generative adversarial networks. *IEEE International Symposium on Biomedical Imaging (ISBI'18)* (2018)

21. Duan, L., Yuan, G., Gong, L., Fu, T., yang, X., Chen, X., Zheng, J.: Adversarial learning for deformable registration of brain MR image using a multi-scale fully convolutional network. *Biomed. Signal Procc. Control* **53** (2018) 101562
22. Fan, J., Cao, X., Wang, Q., Yap, P., Shen, D.: Adversarial learning for mono- or multi-modal registration. *Med. Image Anal.* **58** (2019) 1015 – 1045
23. Younes, L.: Jacobi fields in groups of diffeomorphisms and applications. *Q. Appl. Math.* **65** (2007) 113 – 134
24. Arsigny, V., Commonwick, O., Pennec, X., Ayache, N.: Statistics on diffeomorphisms in a Log-Euclidean framework. *Proc. of the 9th International Conference on Medical Image Computing and Computer Assisted Intervention (MICCAI'06), Lecture Notes in Computer Science* **4190** (2006) 924 – 931
25. Zeiler, M.D., Taylor, G.W., Fergus, R.: Adaptive deconvolutional networks for mid and high level feature learning. *ICCV 2011* (2011) 2018–2025
26. Odena, A., Dumoulin, V., Olah, C.: Deconvolution and checkerboard artifacts. *Distill* (2016)
27. Jaderberg, M., Simonyan, K., Zissermann, A., Kavukcuoglu, K.: Spatial transformer networks. *Proc. of Conference on Neural Information Processing Systems (NeurIPS'15)* (2015)
28. Christensen, G.E., Geng, X., Kuhl, J.G., Bruss, J., Grabowski, T.J., Pirwani, I.A., Vannier, M.W., Allen, J.S., Damasio, H.: Introduction to the non-rigid image registration evaluation project (NIREP). *Proc. of 3rd International Workshop on Biomedical Image Registration (WBIR'06)* **4057** (2006) 128 – 135